Water in Contact with a Cationic Lipid Exhibits Bulk-Like Vibrational Dynamics

Ruth A. Livingstone[1†], Zhen Zhang[2,3], Lukasz Piatkowski[2,4], Huib J. Bakker[2], Johannes Hunger[1], Mischa Bonn[1], and Ellen H.G. Backus[1*]

[1] Max Planck Institute for Polymer Research, Ackermannweg 10, 55128 Mainz, Germany

[2] FOM Institute AMOLF, Science Park 104, 1098 XG Amsterdam, The Netherlands

[3] Chinese Academy of Sciences, 1st North St., ZhongGuanCun, HaiDian District, Beijing 100080, China

[4] The Institute of Photonic Sciences, Mediterranean Technology Park, 08860 Castelldefels, Spain

†Current Address: Center for Free Electron Laser Science, DESY, Hamburg

*Corresponding Author, backus@mpip-mainz.mpg.de, +49-6131-379536

Abstract

Water in contact with lipids is an important aspect of most biological systems, and has been termed 'biological water'. We used time-resolved infrared spectroscopy to investigate the vibrational dynamics of lipid-bound water molecules, to shed more light on the properties of these important molecules. We studied water in contact with a positively charged lipid monolayer using surface-specific 2-dimensional sum frequency generation vibrational spectroscopy with sub-picosecond time resolution. The dynamics of the O-D stretch vibration was measured both for pure D_2O and isotopically diluted D_2O under a monolayer of 1,2-dipalmitoyl-3-trimethylammonium-propane (DPTAP). It was found that the lifetime of the stretch vibration depends on the excitation frequency, and that efficient energy transfer occurs between the interfacial water molecules. The spectral diffusion and vibrational relaxation of the stretch vibration was successfully explained with a simple model, taking into account the Förster transfer between stretch vibrations and vibrational relaxation via the bend overtone. These observations are very similar to those made for bulk water, and as such lead us to conclude that water at the positively charged lipid interface behaves similarly to bulk water. This contrasts the behavior of water in contact with negative or zwitterionic lipids, and can be understood by noting that for the cationic lipids, the charge-induced alignment of water molecules results in interfacial water molecules with O-D groups pointing towards the bulk.

Introduction

Interfacial water molecules are vital for, amongst others, biological systems [1], the climate [2], energy production, [3] and heterogeneous catalysis [4]. Disrupting the hydrogen bonding network at the interface leads to high surface tension. Surfactants reduce that surface tension by forming a monolayer at the surface, which provides hydrogen bond acceptors for the water molecules [1]. Lipids are a key class of biological surfactants, which spontaneously form bilayer membranes when in contact with water. Such lipid bilayers constitute the external boundaries of cells and organelles. Water in contact with lipids can be found immediately outside cells; between the lipid bilayers constituting the cell walls; and inside cells close to either the cell walls or nucleus, chloroplast or mitochondrial membranes. The overall function of membranes relies on a subtle interplay between proteins, lipids and interfacial water. Generally speaking, the assembly of lipids into bilayer membranes depends critically on their interaction with water, and lipid hydration plays a crucial role in lipid phase behavior [1]. The interaction between lipids and water clearly not only affects the lipid structure, but also leads to water characteristics that may be different from those of bulk water and other water interfaces.

In bulk studies of water, important information on water dynamics of HOD and D_2O have been obtained using various time-resolved infrared spectroscopic approaches [5-8]. It was found that the vibrational lifetime of the O-D stretch vibration in D_2O is 400 fs, and in HOD is 1.7 ps [8]. When lipids are added to water, NMR studies have shown that the mobility of lipid-bound water is two orders of magnitude lower than that of bulk water [9-11]. Likewise, dielectric relaxation studies have revealed that the reorientational dynamics of lipid-bound water are greatly slowed down [12-13]. In contrast, the rate of vibrational energy dissipation has been shown to speed up for some types of lipid-bound water. This finding was attributed to the strong coupling of water molecules to the lipid head groups and to additional relaxation pathways present if water is bound to the lipid [14-17]. Most of the previous work has been performed on water in contact with negatively charged or zwitterionic lipids as these are more commonly present in biological systems. A recent interesting study on water in contact with positively charged surfactants [18] has shown indications that the dynamics are similar to the dynamics of bulk water. However, the focus in that paper was on spectral lineshapes. Here, to disentangle the role of the headgroup charge on the water dynamics, we have studied water in contact with a monolayer of positively charged lipids and focus specifically on the vibrational dynamics over a large dynamic range. By comparing this to other studies we can draw conclusions on the effect of interfacial charge on biological water.

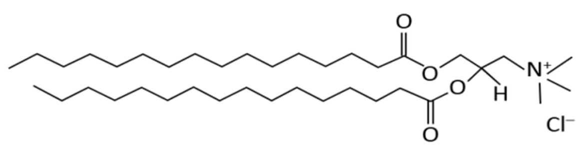

Figure 1: DPTAP molecule

In this study we used surface-specific, time-resolved 2-dimensional infrared spectroscopy to elucidate the dynamics of water interacting with a monolayer of the positively charged lipid 1,2-dipalmitoyl-3-trimethylammonium-propane (DPTAP, Avanti Polar Lipids, figure 1). All experiments were performed at a surface tension around 25 mN/m, which is close to physiological conditions [19-20].

To specifically detect the interfacial water molecules, we employed surface specific vibrational sum frequency generation (SFG) spectroscopy. We measure the intensity spectrum, and ultrafast changes to the intensity spectrum. SFG spectroscopy is a second-order nonlinear optical technique in which visible and infrared laser pulses are overlapped in space and time at an interface. Through their interaction with the surface, emission at the sum of the two frequencies can occur. This sum frequency emission has two important properties: firstly, because the process is forbidden in centro-symmetric media like bulk water, the emission is restricted to the region for which the macroscopic symmetry is broken, typically less than ~10 Å from the interface for lipids [21]; secondly, the emission increases in intensity when the infrared frequency is resonant with a vibration of surface molecules. As a result, SFG spectroscopy provides the vibrational spectrum of the outermost molecular layer(s).

For water in contact with a lipid or surfactant monolayer, static SFG spectroscopy has been used to obtain important insights into the interfacial structure and orientation of water. In both intensity [22-31] and phase-resolved static SFG measurements [32-34], as well as in theoretical studies [21, 26, 35], different types of water molecules have been identified. The structure and arrangement of water molecules next to a lipid monolayer is sensitive to the charge of the headgroup [27, 29, 32, 35]. The charge aligns the water molecules, with negatively (positively) charged lipids causing the water molecules to align with their hydrogen atoms pointing towards (away from) the interface. For negatively charged lipids two types of water have been identified [31], those molecules which are influenced by the negatively charged head-group, and those which are influenced by the bulk water. For zwitterionic lipids (lipids containing both positive and negative charges in their headgroup), up to three types of water have been identified [24, 26, 34]. These have been variously assigned to those influenced by the positive charge, those influenced by the negative charge, those influenced by the hydrophobic tail, and those influenced by the bulk water [21, 24, 34]. The presence of these different types of water is altered by the presence of a carbonyl group in the lipid [26]. It is clear that headgroup charge and composition has a strong influence on interfacial water behavior, although more study is required to obtain a consensus on these effects.

Experimental Methods

Sum frequency spectroscopy techniques

The experimental setup and data analysis has been described in detail elsewhere [31]. Briefly, the sum frequency signal was generated by overlapping a narrowband (15 cm^{-1} FWHM) visible (792 nm) beam on the water sample with a broadband (550 cm^{-1} FWHM) infrared (2300 cm^{-1}) beam. The visible and infrared beams were combined in the sample to create a sum frequency (670 nm) beam, which was detected by a charge coupled device (CCD) camera in reflection geometry from the water surface . In order to measure the time-resolved (2D) spectra, an additional p-polarized narrowband (80 cm^{-1} FWHM) infrared excitation beam with tunable frequency (variously 2230, 2290, 2330, 2380, 2420, 2460, 2500, 2550, and 2620 cm^{-1}) was added. The power of these beams were 15 μJ, 5 μJ and 0.2-7 μJ, and the angles from normal were 70^{o}, 40^{o} and 55^{o} for the visible, infrared and excitation beams respectively. To compare the SFG signal with and without excitation, a chopper was used to block every second excitation pulse, reducing the frequency of the pulses from 1000 Hz to 500 Hz. A mirror that vibrated at 500 Hz was then used to separate in height the two spectra (excited and not excited) on the CCD camera. The difference between the intensity of these two spectra is a measure of what molecules have been excited, and how that population changes as a function of time after excitation. The time between excitation and detection was varied between -2 ps and +20 ps and measurements were taken at 27 different time points in this range. The system response function (cross correlation) was 300 fs FWHM. The experiment was conducted several times to ensure reproducibility. The data were normalized by the excitation beam intensity and by dividing the spectra by the nonresonant SFG signal collected on quartz to account for the detection bandwidth and beam intensity. Our 2D spectra depict the difference of the pumped ($\left|\chi^{(2)}+\chi^{(4)}\right|^2$) and unpumped ($\left|\chi^{(2)}\right|^2$) spectra, i.e. essentially the term $\chi^{(2)}\times\chi^{(4)*}+\chi^{(2)*}\times\chi^{(4)}$, given that the $\left|\chi^{(4)}\right|^2$ term is very small.

Sample preparation

DPTAP lipid powder was used as received from Avanti lipids. A solution of 0.075 mg/ml DPTAP in chloroform was dropped on the surface of the water. The chloroform evaporated, leaving behind a monolayer of lipids. The surface pressure of the water was measured as the drops were added, until a surface pressure of 25 mN/m was obtained. Water was added from a reservoir as it evaporated, to keep the height stable throughout the measurement. This water was added from the side of the trough, below the surface, to avoid disturbing the lipid monolayer. The IR laser pulses damaged the lipids over time, leading to a reduction in surface pressure. To reduce this effect, the laser pulses were defocussed, a rotating trough was used, and additional lipids were dropped on the surface during the course of the experiment to keep the surface pressure within 25 ± 5 mN/m.

Results and discussion

SFG spectra of water under a positively charged lipid monolayer (DPTAP) at three different isotopic dilutions (H_2O:HOD:D_2O = 0:0:1; 1:2:1 and 5:4:1) are depicted in figure 2 for SSP polarization (SFG S, visible S, infrared P). As has been previously discussed [36], upon isotopic dilution the two spectral features merge into one and the spectrum becomes narrower. This has been explained by the two spectral features originating from a Fermi resonance with the bending overtone, which causes splitting of the O-D stretch feature. The bending mode of D_2O has roughly half the frequency of the OD stretching mode. However in HOD the bending vibration shifts, so this resonance disappears and the spectrum collapses into one peak. Intermolecular coupling could also contribute substantially to the peak splitting [37].

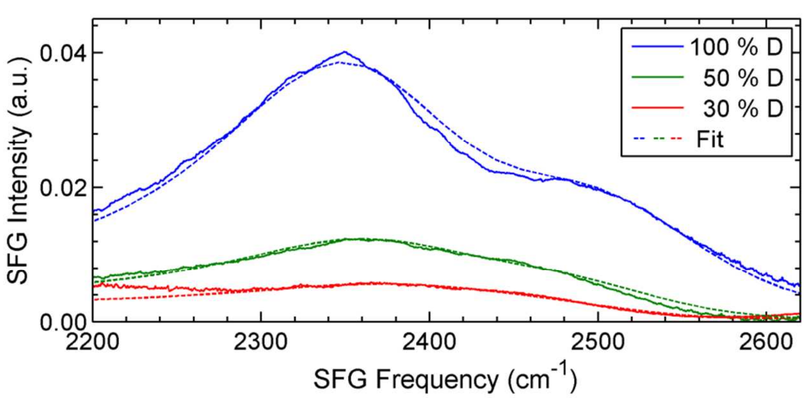

Figure 2: Static experimental (solid) and modelled (dotted) SFG spectra for pure D_2O (blue) and isotopically diluted water (green); H_2O:HOD:D_2O = 1:2:1, (red); H_2O:HOD:D_2O ≈ 5:4:1) under a monolayer of DPTAP lipid at a surface pressure of 25 mN/m, in the OD stretch region.

The large width of even the isotopic diluted spectra indicates that, as similar to bulk water, the water molecules have a large distribution in hydrogen bond strengths. Moreover, compared to water at the water/air interface [36], the static spectra show more intensity at low frequencies than at high frequencies, suggesting that the water molecules underneath DPTAP are on average more strongly hydrogen bonded. In addition, the water signal is enhanced by the addition of the DPTAP monolayer, suggesting that the interfacial water molecules are aligned by the charge of the lipid headgroup. This effect has been widely seen in literature for charged surfactants and lipids [32, 38].

Although the static SFG spectra contain valuable information about the alignment and hydrogen-bonding conditions of the interfacial water, no information about the energy relaxation and/or structural dynamics of these molecules can be obtained. Time-resolved two dimensional SFG (tr-2DSFG) [39-42] can give information on the vibrational lifetimes and energy transfer dynamics and pathways. This technique has been applied to the water-air interface [40, 43-44], and the water-surfactant interface [18, 31]. It was found that for the water-air interface the energy relaxation is slower than for bulk water [45], due to the reduction of the density of acceptor molecules for intermolecular energy transfer [40]. The mechanisms of energy relaxation, however, were concluded to be the same as in bulk water [45].

When a negatively charged surfactant is added to the water-air interface, the interfacial water molecules look very different [31]. The interfacial water consists of two distinct sub-ensembles: water molecules with localized vibrations, influenced by the negatively charged surfactant; and water molecules with delocalised vibrations, influenced by the bulk water molecules. These two ensembles are coupled, and can exchange vibrational energy. The energy relaxation mechanism for the second, bulk-like group was seen to be the same as observed in bulk water. On the other hand, with a positively charged surfactant present at the interface, the shape of the 2D spectra could be explained using a single type of interfacial water molecules [18], which is similar to the shape of the air-water interface in the hydrogen-bonded region [40]. This suggests that positively charged surfactants have less influence on the hydrogen bonding network of water than negatively charged surfactants. There has been no detailed study, however, on the energy relaxation dynamics and coupling of water at a positively charged surfactant. In addition, previous tr-2DSFG studies have focused on industrial surfactants, not on lipids. In the present study we perform tr-2DSFG on the water-positively charged lipid interface, to explore the energy transfer dynamics and the interaction between water and lipid molecules.

To obtain this information we use a relatively narrow band (~80 cm^{-1}) tunable infrared excitation pulse to excite a subset of water molecules to the vibrational excited state. Subsequently, at certain delay times after the excitation pulse, the SFG detection (infrared and visible) pulse pair measures the response of the interfacial molecules to the excitation. As the infrared pulse from the detection pair is broadband, the whole O-D stretch water band can be detected simultaneously. By varying the frequency of the infrared excitation pulse a full 2D spectrum can be obtained. Figure 3 depicts 2D spectra of water in contact with DPTAP (at a surface pressure of 25±5 mN/m) on D_2O [46] and isotopically diluted D_2O at selected times after excitation. We measured D_2O instead of H_2O to make use of the longer lifetime of the O-D stretch vibration compared to O-H. The spectra shown are the difference between excited and ground state 2D spectra, with P-polarized excitation pulse and SSP-polarized detection. At long times, following vibrational relaxation and energy redistribution, the energy in the excitation pulse causes heating of the sample (typically by a few degrees) and thermal effects can distort the 2D spectra, as the heated sample has a blue-shifted spectrum. Thus upon taking the difference between the excited (hot) and ground state (cold) spectrum, the blue (red) side trivially shows a positive (negative) difference at long times after excitation. We corrected for these heating effects in the 2D spectra shown in figure 3 by correcting the data with an appropriate model of these effects. Commonly D_2O relaxation is described by relaxation with a time constant of 400 fs [8] for decay to an intermediate state and 700 fs [31] for relaxation from this intermediate state to the hot ground state. In order to approximate the ingrowth of the hot ground state, an exponential ingrowth (τ = 1 ps) convolved with the system response was used. The response of the heated sample was taken from the difference spectra at a later (10 ps) time after excitation. The 2D spectra without the heat correction can be found in the supplementary information. Details about how the 2D spectrum was measured, constructed and corrected for heat can be found in [31].

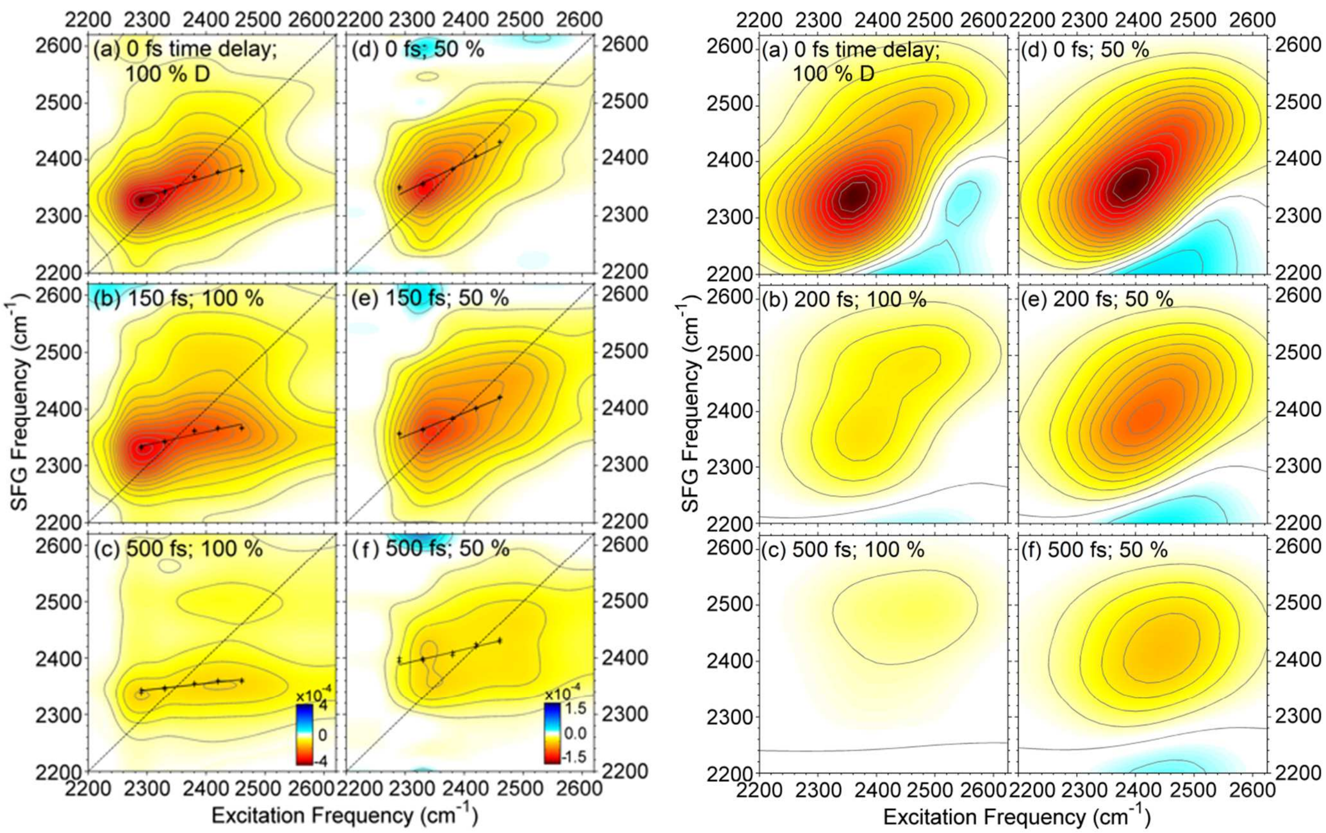

Figure 3: Left: tr-2DSFG spectra (heat corrected) of pure (a-c) and isotopic diluted (d-f) D_2O under DPTAP (H_2O:HOD:D_2O = 1:2:1). The black points with error bars mark the peak bleach at the different excitation frequencies, obtained using a Gaussian fit, and the black line is the linear fit to those points

used to obtain the slope. Note that a signal size of -3 x 10^{-4} (-1.1 x 10^{-4}) corresponds to 15 % bleach for pure D_2O (isotopic diluted D_2O). Right: modelled SFG spectra

The 2D spectra at zero time (all beams are overlapped in time, figure 3(a)) reveals that the overall response is inhomogeneously broadened, as evident from the response being elongated along the diagonal. In addition there is some off-diagonal intensity (crosspeaks), most prominently at the bottom right hand corner (figure 3(a) excitation at 2500 cm^{-1}, detection at 2380 cm^{-1}). This off-diagonal intensity has previously been observed at the cationic surfactant CTAB interface [18], and has been assigned to vibrational coupling between low and high frequency due to the Fermi resonance with the bending overtone that causes as well the spectral features in the static spectra [36]. The combination of the Fermi resonance with the inhomogeneous broadening of the O-D stretch vibration can fully explain the shape of the 2D spectra, as compellingly shown in [18]. The slope of the 2D spectrum (the black lines in figure 3) at zero time after excitation provides a direct measure of the heterogeneity of the OD groups at the surface. For a completely homogeneous surface, the response is independent of the excitation frequency resulting in a zero slope, when the excitation frequency is plotted along the horizontal axis. Inversely, for a completely inhomogeneous surface, only those molecules that are excited will respond, resulting in a slope along the diagonal, i.e. a slope=1. The slope is calculated by fitting Gaussian curves to the raw data that represent various slices through the 2D spectra. The center of the Gaussian indicates the peak bleach at that excitation frequency (see the black points in figure 3). A linear fit to these peak bleach values was used to determine the slope of the spectrum (see black lines in figure 3). The slope at zero time after excitation (figure 3(a)) is 0.34, showing that the water interface is fairly, but certainly not completely, inhomogeneous. The off-diagonal intensity distorts the 2D spectra, which could cause this measure of the inhomogeneity to be somewhat underestimated. Upon isotopic dilution, changing the system from D_2O towards HOD, the 2D spectrum (figure 3(d-f)) simplifies in a similar fashion to the static SFG spectrum (figure 2). The inhomogeneously broadened signal remains along the diagonal but the off-diagonal signal disappears, because the overtone of the bending mode of HOD is no longer in resonance with the OD stretch vibration. The slope for the isotopically diluted sample is slightly higher, at 0.51, which is most likely due to smaller off-diagonal intensity and thus less distortion of the 2D spectrum rather than a more inhomogeneous environment.

The slope decays as the time after excitation increases, as a result of spectral diffusion. The molecules lose memory of their initial excitation frequency. The time-dependent slope of the 2D spectrum reflects the timescale of spectral diffusion. For both pure and isotopically diluted D_2O the time-dependent slope is depicted in figure 4(a). It was found that the slope decayed in 350 fs for the pure D_2O – lipid interface, and 1.1 ps for the isotopically diluted water-lipid interface (dotted lines in figure 4(a)). A decay of the inhomogeneity could occur either due to structural relaxation or intermolecular energy transfer. For the water-air interface it has been concluded that intermolecular energy transfer was the dominant relaxation mechanism [40, 45], which could be well described with the Förster model. This model [40, 47] describes dipole-dipole coupling between different molecular groups, in our case O-D groups. As this coupling can occur between O-D groups with slightly different frequencies, the frequency-frequency correlation function will decay and the slope will decay accordingly. Upon isotopic dilution the distance between vibrational energy donor and acceptor on average becomes larger, slowing down the Förster transfer [40]. As shown recently [47], for Förster transfer at an interface the original Förster model has to be modified from a spherical to a hemispherical geometry, as shown here:

$$S(t) = S_0 \exp\left(-\frac{2}{3}\pi^{\frac{3}{2}} C_{OD} N_A \sqrt{\frac{r_0^6 t}{\tau_1}}\right) \qquad (1)$$

Where S_0 is the initial slope, N_A is Avogadro's constant, r_0 is the Förster radius, i.e. the distance at which the energy transfer occurs with 50 % efficiency within a vibrational lifetime. Excluded volume effects are not considered here [48]. Here we use the Förster radius r_0 of 2.1 Å [47] with a corresponding time period τ_1 of 1.7 ps previously determined for bulk D_2O [8]. The concentration of OD oscillators C_{OD} is 110.6 mol^{-1} for pure D_2O [47] and 55.3 mol^{-1} and 33.18 mol^{-1} for the isotopic dilutions H_2O:HOD:D_2O = 1:2:1 and 5:4:1 respectively. The outcome of this model convoluted with the system response function is shown as the solid lines in figure 4(a). Note that the lines are not fits; beside the initial slope (S_0 = 0.4 for pure D_2O and 0.55 for 50 % isotopic dilution), there are no adjustable parameters. The off-diagonal signal described above (the result of Fermi resonance with the bending mode of D_2O) has the same vibrational relaxation pathways and energy transfer lifetime as the diagonal signal. This means that the distortions will only affect the initial slope S_0 in the equation but not the slope decay. To verify that this model provides a good description of our system, we determined the spectral diffusion after excitation at 2290 cm^{-1} (figure 4(b)), which also represents the inhomogeneity of the molecules [42, 49]. The spectral diffusion is measured by observing the peak bleach frequency after excitation with a 2290 cm^{-1} pulse as a function of time after excitation. The peak bleach is determined by fitting with a Gaussian curve and taking the center of that curve. The bleach frequency is also seen to agree with the Förster model (the scaled and offset model is plotted as solid lines in figure 4(b)). So, in two different quantities we find the same decay behavior reflecting the time-dependent decrease in inhomogeneity of the system.

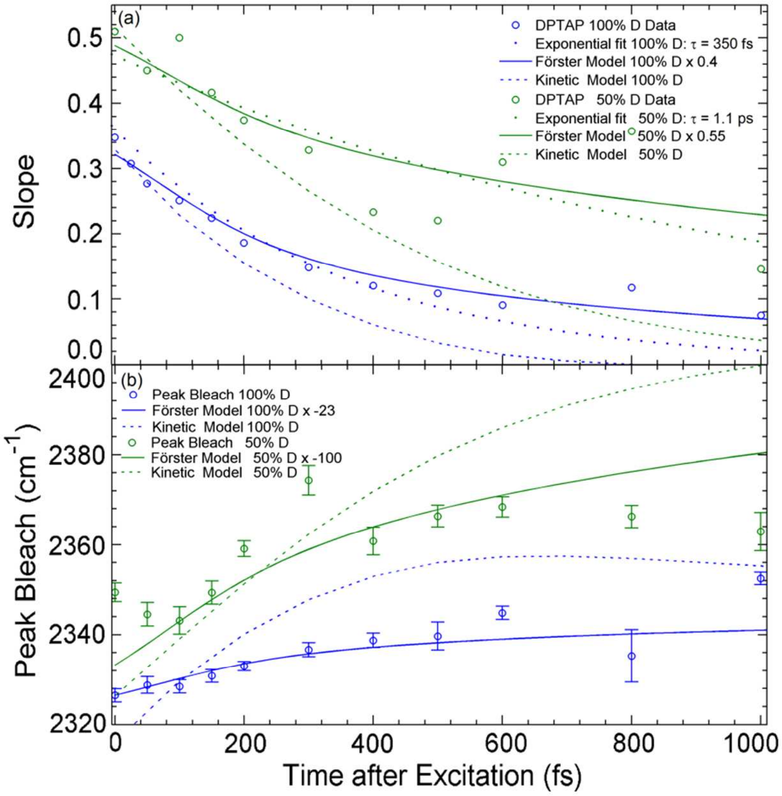

Figure 4: (a) Slope of the 2D diagonal response, and (b) spectral diffusion dynamics after exciting at 2290 cm^{-1}, both as function of time after excitation. Measurements with pure D_2O are shown as blue circles and those with isotopically diluted D_2O are shown as green circles; both are under a DPTAP monolayer. The solid lines show the result of the Förster model convolved with the system response function, which describes the data remarkably well. Note that these lines are not fits: the only adjustable parameters are scaling factors (indicated in legends), and an offset factor in the case of the bleach (2320 cm^{-1}). The blue and green dashed lines are the time-dependent slope, bleach and width calculated using the kinetic model schematically depicted in figure 6. From the simulations, the slope has been determined between 2300 and 2450 cm^{-1}, and 2300 and 2500 cm^{-1} for pure and isotopically diluted D_2O, respectively. . The dotted lines in (a) are single-exponential fits.

Fast spectral diffusion has also been observed for isotopically diluted water (H_2O in D_2O) under a positively charged surfactant (CTAB) by measuring 2D phase-resolved (i.e. heterodyne) detected sum-frequency generation spectra. Inoue et al [18] showed that a Fermi-resonance causes splitting of the OH stretch vibration, leading to off-diagonal intensity in the 2D spectra. In agreement with our data, they found that the inhomogeneity of the interfacial water is no longer prominent at 300 fs [18, 41]. However the number of measured data points in time was somewhat limited in that study, making a full analysis of the water dynamics at this comparable interface somewhat challenging.

2D infrared spectra have been measured for water inside reverse micelles of surfactants [50]. In such a micelle, part of the water is in contact with the surfactant, as in the case of a monolayer of surfactant on top of water. Very small micelles are believed to be a good model for interfacial water [50]. Interestingly, the shape of the 2D spectrum for isotopically diluted water (D_2O in H_2O) inside a small negatively charged AOT micelle looked qualitatively similar to the 2D SFG spectrum presented in figure 3(d-f). Please note that we compare our squared $|\chi^{(2)}|^2$ difference spectrum (i.e. pump on minus pump off), as defined in the experimental section, with the 2D IR spectrum, while in principle the imaginary difference $\chi^{(2)}$ spectrum should be compared. Since the water molecules are aligned by the lipid charge with their hydrogen atoms pointing towards the bulk, the imaginary $\chi^{(2)}$ spectrum is entirely negative in the O-D stretch region. Apart from the imaginary $\chi^{(2)}$ spectrum having a distinct sign, the shape of the imaginary $\chi^{(2)}$ spectrum closely resembles the shape of the $|\chi^{(2)}|^2$ spectrum (see SI for more information). Considering that there is no significant dissimilarity between the different ways of measuring, it can be demonstrated that any artefacts introduced by measuring the difference in $|\chi^{(2)}|^2$, rather than the imaginary $\chi^{(2)}$ SFG signal are not large enough to affect our analysis or conclusions. However, please note that the discussion above regarding 2D lineshapes and the discussion below about the lifetime, relies on the assumption that the difference in intensity spectra (homodyne detection) can be interpreted the same as the difference of imaginary $\chi^{(2)}$ spectra (heterodyne detection). A detailed, quantitative comparison that shows this assumption to be largely correct, is outside the scope of the current manuscript and will be the subject of a further publication.

It is interesting to compare our interfacial 2-D spectra observed for water in contact with positively charged monolayer to interfacial 2-D spectra previously reported for negatively charged monolayers. For the negatively charged surfactant/lipid, the O-D/O-H groups of the water molecules are pointing with the D/H atom towards the surfactant/lipid. Water that is hydrogen bonded to the lipid is found to be more isolated from bulk water, and thereby display a slower relaxation time [31]. Water molecules in contact with zwitterionic lipids show predominantly O-D/O-H groups pointing to the surfactant/lipid [24, 26, 51], making the dynamics similar to the negatively charged case as observed by Costard et al [52]. For the positively charged lipids the O-D/O-H vibration of the water molecules point away from the lipids (with the O atom pointing towards the positive charge) and are thus in direct contact with bulk water. The dynamics may then be expected to be mostly determined by bulk water, accounting for the faster energy transfer observed previously for water in contact with CTAB [18, 41] and for water underneath DPTAP as described in the present work.

To test the hypothesis that interfacial water molecules in contact with a cationic lipid layer behave like bulk water, we investigated the vibrational relaxation of the interfacial water molecules. If the water interacts significantly with the lipid, one would expect that those water molecules that are interacting with the lipid would have different dynamics to those interacting mainly with other water molecules, as has been observed for the negatively charged interface [31]. If, however, the positively charged lipid has little influence on the interfacial water one would expect the water dynamics to be similar to that of bulk water or, perhaps more appropriately, the air-water interface.

The 2D spectra contain this information about the vibrational relaxation pathways. In order to extract this information, the bleach intensity was monitored as a function of time after excitation at certain selected excitation and detection frequencies. Figure 5 (a) shows how the bleach changes as a function of time after excitation for two selected excitation wavelengths and three isotopic dilutions. For each of these traces, the bleach was averaged over 50 cm^{-1} region of the SFG spectrum, centered at the excitation frequency. At long times after excitation an offset can be seen. This offset is due to the thermal effects described above.

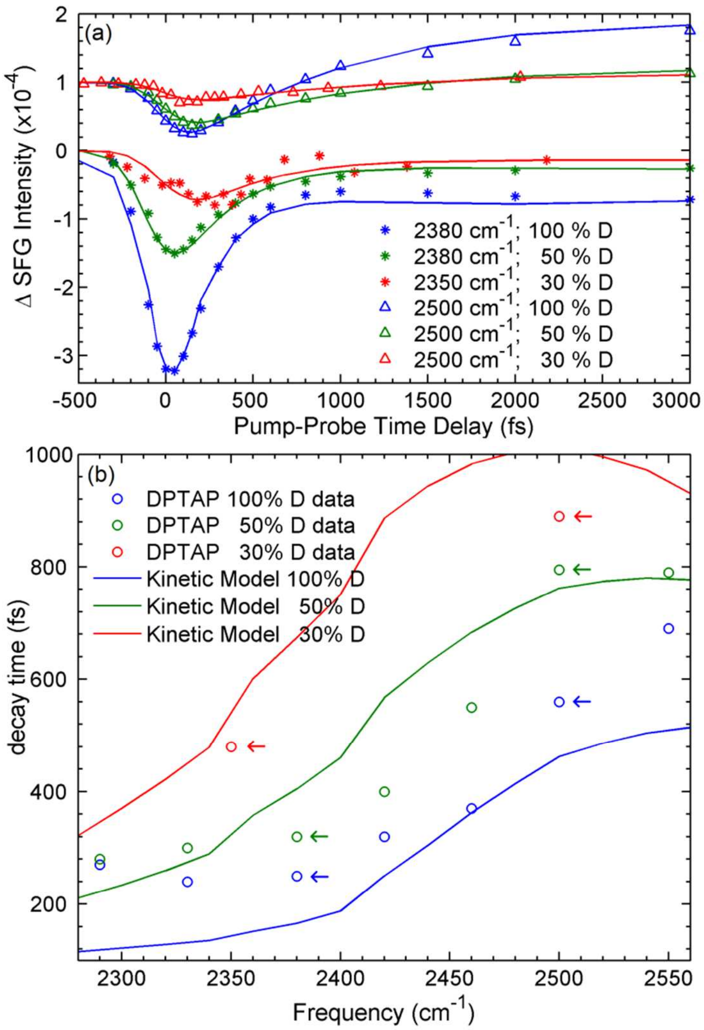

Figure 5: Frequency dependent decay times for different degrees of isotopic dilution indicated in the graph. The data were fitted with a four level differential equation model with time constants τ_{eq} = 700 fs and τ_1. The raw data and corresponding fits at two of the excitation frequencies and the three different isotopic dilutions are shown in (a). The τ_1 values extracted from the fits are plotted in (b), where a clear frequency dependence of the lifetime is observed. This frequency dependence can be modelled (solid lines) by accounting for Förster transfer between stretch vibrations, and vibrational relaxation via the bend overtone. The τ_1 values in (b) extracted from the fits shown in (a) are highlighted by arrows.

The fits not shown in (a) can be found in the supplementary information. See text for more details on the fitting and the model.

To model the water dynamics and extract the relaxation lifetime we used a set of four coupled differential equations. The water molecules are excited from the ground state to the vibrationally excited (O-D stretch) state by the excitation pulse. The molecules then relax to an intermediate state with a time constant τ_1. This intermediate state likely has the excitation in the D_2O bending mode [53]. The SFG spectrum in the OD stretch region with excited bend vibration is assumed to be the same as the ground state spectrum [54]. From the intermediate state the molecules relax to a hot ground state with a fixed timescale τ_{eq} = 700 fs [31]. This model has previously been used to describe water dynamics [31, 55-56], and a full description can be found in the supplementary information. It can be seen from figure 5 that, on average, the τ_1 lifetime is similar to the 400 fs lifetime that has been measured in bulk D_2O [8]. However, relaxation times as a function of frequency are observed to differ by a factor of >3. With increasing frequency the lifetime increases, in agreement to what has been seen in other studies of water [45, 57]. This has been attributed to the stronger coupling to the bending mode of stretch vibrations at lower frequencies compared to those at higher frequencies[45]. The bend vibration of D_2O lies at around 1203 cm^{-1} (measured using Attenuated Total Internal Reflection Infra-red Spectroscopy (ATR)). The anharmonicity of the bend overtone in HOD is known to be around 45 cm^{-1} [58]. Assuming the anharmonicity is the same in the D_2O bend, the overtone should lie at around 2361 cm^{-1}. The overlap of the bend overtone with the stretch vibration allows the water molecules to rapidly relax after excitation of the stretch mode. This overlap is strongest, and so the relaxation is fastest, for those water molecules with stretch vibrations close to 2361 cm^{-1}.

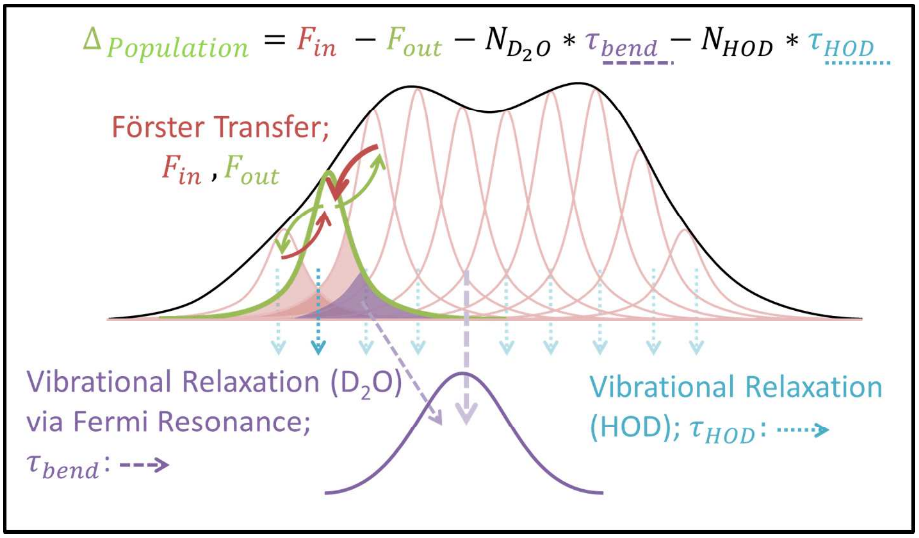

Figure 6: Schematic depiction of the model: for a specific sub-ensemble of OD oscillators (highlighted in green) on the red side of the inhomogeneous distribution of oscillators, (de-)population occurs by exchange between nearby sub-ensembles through near-resonant Förster energy transfer (curved arrows). The efficiency of Förster energy transfer is given by the spectral overlap between the different sub-ensembles (shaded pink regions). Depopulation of the state further occurs by two mechanisms: (i) vibrational relaxation by coupling between the stretch and bending mode overtone (purple dashed arrows) the spectrum of the latter is schematically depicted below the stretch mode). The efficiency of this relaxation channels is determined by the spectral overlap between the stretch mode and the bend overtone spectrum (shaded purple region); and (ii) 'simple' vibrational relaxation (light blue dotted lines), which occurs preferentially for isotopically diluted HOD molecules, for which the bending mode is not degenerate with the OD stretch.

The frequency dependent lifetime of the water stretch vibration has previously been observed and modelled for H_2O in the bulk and at the water-air interface [45]. Here we use the principles of that model to calculate the time-dependent 2D-SFG spectra from which we subsequently infer the slope decay and the frequency dependent lifetime similar to what has been done in the experiments. 2D-SFG spectra are calculated as described in Ref [59], assuming a Lorentzian distribution of oscillators spaced by 25 cm^{-1}

between 2000 and 3000 cm^{-1} with a FWHM of 106 cm^{-1}, by analogy to the FWHM of 150 cm^{-1} used for H_2O in Ref [45]. The intensity of every Lorentzian is determined by a double Gaussian distribution, each with a peak width of 90 cm^{-1} and central frequencies varying for the different fraction isotopic dilution such that the resulting model accurately describes the static experimental data. The resulting static SFG spectrum is the square of the sum of all 41 Lorentzians and a nonresonant contribution with the same phase and amplitude for the three different samples (see Fig. 2 dotted lines). The 2D SFG spectra at time zero are calculated from the overlap integral between the 80 cm^{-1} FWHM Gaussian excitation pulse and each Lorentzian and normalizing to a maximum bleach of 10 %. The anharmonicity between the ground state and first excited state is set to 150 cm^{-1} [60-62]. Similar to the experiments, the simulated 2D SFG spectra are calculated as the difference between the pumped and unpumped spectra. Subsequently, the time evolution of the 2D spectra has been obtained with the model graphically depicted in Fig. 6. Briefly, this model takes into account spectral diffusion through Förster transfer and vibrational relaxation through coupling to the bending overtone. Spectral diffusion was assumed to be caused entirely by energy transfer between the different Lorentzian oscillators with a rate proportional to the frequency overlap of different Lorentzian oscillators. Vibrational relaxation to the ground state was assumed to occur through the D_2O bend overtone. The bend overtone in D_2O is modelled by a Gaussian with a full width at half maximum (FWHM) of 58 cm^{-1} (from the ATR spectra) and centered at 2361 cm^{-1} (see justification above). The vibrational relaxation rate is calculated from the overlap integral between the overtone spectrum and the Lorentzian describing a certain the oscillator. The frequency dependence of the transition dipole was taken into account throughout the whole calculations to convert spectral intensity into population and in the overlap integrals as explained in Ref. [45]. In an iterative process, the Förster rate and the vibrational relaxation rate, used to normalize the rates calculated through the overlap integrals, are chosen to describe simultaneously the frequency dependent lifetime, the slope decay, and the spectral diffusion at 2290 cm^{-1} for pure D_2O and two isotopic dilutions (see below). The system of coupled differential equations has been solved for every 0.1 ps between 0 and 1 ps following Ref [63], resulting in the time-dependent populations. From these time-dependent populations the 2D spectra at selected time points are calculated (right panel of Fig. 3). Subsequently, using the same methodology as for the experimental data, the slope decay, spectral diffusion, and frequency dependent lifetime are obtained from the 2D spectra. For the slope decay and the spectral diffusion a double Gaussian distributions has been fit to vertical slices through the spectrum. The peak maximum of the lowest frequency Gauss has been used to determine the slope and the spectral diffusion. The lifetime has been obtained by integrating the vertical slice over 90 cm^{-1} symmetrically along the diagonal. The results are shown in Fig. 4 and 5 and show a reasonable agreement with the data for pure D_2O.

The applicability of the kinetic model can be further tested by extending it to model isotopically diluted water. The observed longer lifetime for HOD compared to D_2O has previously been reported for bulk D_2O: pure D_2O shows a vibrational lifetime of ~400 fs [8], while for an isolated OD oscillator in H_2O lifetimes around 1.7 ps have been reported [8]. By changing to HOD the bending mode vibrates at 1420 cm^{-1} [58] (overtone = 2795 cm^{-1}), while the O-D stretch vibration remains at the same frequency. This results both in the simplification of the static SFG spectrum as the Fermi resonance is now absent (figure 2) and in less efficient energy relaxation, i.e. longer relaxation times (figure 5). In the 50 % D isotopically diluted experiment (H_2O:HOD:D_2O = 1:2:1), there are an equal number of O-D oscillators coming from D_2O and from HOD. The frequency dependence of the lifetime is therefore expected to remain, but the lifetime should be longer at all frequencies. In figure 5 the green points show that the 50 % D lifetimes are consistently around 30 % longer. When the isotopic dilution is extended further to 30 % D (H_2O:HOD:D_2O ≈ 5:4:1) the lifetime becomes even closer to that of an isolated OD oscillator in bulk D_2O, around 60 % longer (red points in figure 5). The model used to describe the pure D_2O was modified to account for isotopic dilution by assuming two sub-ensembles of OD groups: those that are in

HOD molecules, relaxing at a constant rate of 1.7 ps [8], and those in D_2O molecules, which relax via the Fermi resonance as before. Förster transfer can occur between the different types of molecules. Compared to pure D_2O, the Förster transfer rates between the different Lorentzians were multiplied by 0.5 and 0.3 for 50 % D_2O and 30 % D_2O, respectively, to account for the reduced density of OD groups. The results of this model are shown as the solid red and green lines in Figure 5, and describe the measured data well. Note, that the three samples, 100, 50, and 30 % D_2O, are modelled with the same set of parameters reproducing the whole set of experimental data remarkably well. The discrepancies between model and experimental could partly be explained by the observation that the Fermi resonance leads to population transfer, immediately after excitation, to the two peaks seen in the static spectrum. This effect leads to the off-diagonal signal seen in the 2D spectrum, which was not accounted for in the kinetic model. The effect is most pronounced for the pure D_2O. However, the model captures the essence of the energy relaxation processes. As this model is the same model as used to successfully describe water dynamics in bulk and the water-air interface, there is a strong indication that the water molecules underneath the lipid have the same relaxation pathways as water in the bulk and at the air interface – i.e. the presence of the positively charged lipid does not significantly affect the water vibrational dynamics. This conclusion is in agreement with a recent study on hydrated bilayers of the lipid DMTAP [64] and charged lipids on water [65].

Conclusions

In all cases it can be seen that the simple kinetic model based on only the established dynamics of pure water can reproduce the essentials of the 2D time-resolved data measured on water under a DPTAP monolayer. The frequency dependence of the lifetime, the slow-down upon isotopic dilution, and the agreement with the theoretical model all support our conclusion that the stretch vibration relaxes via the bend vibration. These conclusions are consistent with bulk water and water at the water/air interface. They suggest that the interaction of the positively charged lipid monolayer with the water molecules does not lead to a fundamental difference in the water vibrational dynamics, unlike what has been observed at the negatively charged surfactant interface [31]. As such, we conclude that water in the water/cationic lipid interface behaves in a fashion very similar to bulk water, in terms of its vibrational dynamics. This can be understood by noting that the water oxygen atom are attracted to the positive charge in the lipid, so that the OH is pointing down into the water phase, behaving as if it were part of that water structure. These conclusions help us to disentangle the role of the headgroup charge from the role of the rest of the lipid in influencing the biological water dynamics.

Supporting Information. Phase-resolved SFG data, four level model, and two-dimensional SFG spectrum without heat subtraction. This information is available free of charge via the Internet at http://pubs.acs.org

Acknowledgements

The authors thank M.-J. van Zadel and H. Schoenmaker for excellent technical support. RAL thanks the Alexander von Humboldt Foundation. Some of this work was conducted as part of the research program of the "Stichting voor Fundamenteel Onderzoek der Materie (FOM)" which is financially supported by the "Nederlandse organisatie voor Wetenschappelijk Onderzoek (NWO)".

References

1. Milhaud, J., New Insights into Water-Phospholipid Model Membrane Interactions. *Biochim. Biophys. Acta, Biomembr.* **2004**, *1663*, 19-51.
2. Haji-Akbari, A.; DeFever, R. S.; Sarupria, S.; Debenedetti, P. G., Suppression of Sub-Surface Freezing in Free-Standing Thin Films of a Coarse-Grained Model of Water. *Phys. Chem. Chem. Phys.* **2014**, *16*, 25916-25927.
3. Chung, T.-S.; Li, X.; Ong, R. C.; Ge, Q.; Wang, H.; Han, G., Emerging Forward Osmosis (FO) Technologies and Challenges Ahead for Clean Water and Clean Energy Applications. *Curr. Opin. Chem. Engin.* **2012**, *1*, 246-257.
4. Pruden, A. L.; Ollis, D. F., Photoassisted Heterogeneous Catalysis: The Degradation of Trichloroethylene in Water. *J. Catal.* **1983**, *82*, 404-417.
5. Asbury, J. B.; Steinel, T.; Kwak, K.; Corcelli, S. A.; Lawrence, C. P.; Skinner, J. L.; Fayer, M. D., Dynamics of Water Probed with Vibrational Echo Correlation Spectroscopy *J. Chem. Phys.* **2004**, *121*, 12431-12446.
6. Asbury, J. B.; Steinel, T.; Stromberg, C.; Corcelli, S. A.; Lawrence, C. P.; Skinner, J. L.; Fayer, M. D., Water Dynamics: Vibrational Echo Correlation Spectroscopy and Comparison to Molecular Dynamics Simulations. *J. Phys. Chem. A* **2004**, *108*, 1107-1119.
7. Steinel, T.; Asbury, J. B.; Corcelli, S. A.; Lawrence, C. P.; Skinner, J. L.; Fayer, M. D., Water Dynamics: Dependence on Local Structure Probed with Vibrational Echo Correlation Spectroscopy *Chem. Phys. Lett.* **2004**, *386*, 295-300.
8. Piatkowski, L.; Eisenthal, K.; Bakker, H., Ultrafast Intermolecular Energy Transfer in Heavy Water. *Phys. Chem. Chem. Phys.* **2009**, *11*, 9033-9038.
9. Zhou, Z.; Sayer, B. G.; Hughes, D. W.; Stark, R. E.; Epand, R. M., Studies of Phospholipid Hydration by High-Resolution Magic-Angle Spinning Nuclear Magnetic Resonance *Biophys. J.* **1999**, *76*, 387-399.
10. Kurze, V.; Steinbauer, B.; Huber, T.; Beyer, K., A ^{2}H NMR Study of Macroscopically Aligned Bilayer Membranes Containing Interfacial Hydroxyl Residues. *Biophys. J.* **2000**, *78*, 2441-2451.
11. Gawrisch, K.; Gaede, H. C.; Mihailescu, M.; White, S. H., Hydration of POPC Bilayers Studied by ^{1}H-PFG-MAS-NOESY and Neutron Diffraction. *Eur. Biophys. J. Biophys. Lett.* **2007**, *36*, 281-291.
12. Klosgen, B.; Reichle, C.; Kohlsmann, S.; Kramer, K. D., Dielectric Spectroscopy as a Sensor of Membrane Headgroup Mobility and Hydration. *Biophys. J.* **1996**, *71*, 3251-3260.
13. Tielrooij, K. J.; Paparo, D.; Piatkowski, L.; Bakker, H. J.; Bonn, M., Dielectric Relaxation Dynamics of Water in Model Membranes Probed by Terahertz Spectroscopy. *Biophys. J.* **2009**, *97*, 2484-2492.
14. Zhao, W.; Moilanen, D. E.; Fenn, E. E.; Fayer, M. D., Water at the Surfaces of Aligned Phospholipid Multibilayer Model Membranes Probed with Ultrafast Vibrational Spectroscopy *J. Am. Chem. Soc.* **2008**, *130*, 13927-13937.
15. Bonn, M.; Bakker, H. J.; Ghosh, A.; Yamamoto, S.; Sovago, M.; Campen, R. K., Structural Inhomogeneity of Interfacial Water at Lipid Monolayers Revealed by Surface-Specific Vibrational Pump-Probe Spectroscopy. *J. Am. Chem. Soc.* **2010**, *132*, 14971-14978.
16. Gruenbaum, S. M.; Skinner, J. L., Vibrational Spectroscopy of Water in Hydrated Lipid Multi-Bilayers. I. Infrared Spectra and Ultrafast Pump-Probe Observables *J. Chem. Phys.* **2011**, *135*, 075101.
17. Piatkowski, L.; Heij, J. d.; Bakker, H. J., Probing the Distribution of Water Molecules Hydrating Lipid Membranes with Ultrafast Förster Vibrational Energy Transfer *J. Phys. Chem. B* **2013**, *117*, 1367-1377.
18. Inoue, K.-i.; Nihonyanagi, S.; Singh, P. C.; Yamaguchi, S.; Tahara, T., 2D Heterodyne-Detected Sum Frequency Generation Study on the Ultrafast Vibrational Dynamics of H_2O and HOD Water at Charged Interfaces. *J. Chem. Phys.* **2015**, *142*, 212431.
19. Ege, C.; Lee, K. Y. C., Insertion of Alzheimer Aβ40 Peptide into Lipid Monolayers. *Biophys. J.* **2004**, *87*, 1732-1740.
20. Seelig, A., Local Anesthetics and Pressure: A Comparison of Dibucaine Binding to Lipid Monolayers and Bilayers. *BBA-Biomembranes* **1987**, *899*, 196-204.
21. Nagata, Y.; Mukamel, S., Vibrational Sum-Frequency Generation Spectroscopy at the Water/Lipid Interface: Molecular Dynamics Simulation Study. *J. Am. Chem. Soc.* **2010**, *132*, 6434-6442.
22. Sovago, M.; Vartiainen, E.; Bonn, M., Observation of Buried Water Molecules in Phospholipid Membranes by Surface Sum-Frequency Generation Spectroscopy. *J. Chem. Phys.* **2009**, *131*, 161107.
23. Sovago, M.; E.Vartiainen; Bonn, M., Erratum: "Observation of Buried Water Molecules in Phospholipid Membranes by Surface Sum-Frequency Generation Spectroscopy" [J. Chem. Phys. 131, 161107 (2009)]. *J. Chem. Phys.* **2010**, *133*, 229901.
24. Mondal, J. A.; Nihonyanagi, S.; Yamaguchi, S.; Tahara, T., Three Distinct Water Structures at a Zwitterionic Lipid/Water Interface Revealed by Heterodyne-Detected Vibrational Sum Frequency Generation. *J. Am. Chem. Soc.* **2012**, *134*, 7842-7850.
25. Bonn, M.; Nagata, Y.; Backus, E. H. G., Molecular Structure and Dynamics of Water at the Water–Air Interface Studied with Surface-Specific Vibrational Spectroscopy. *Angew. Chem. Int. Edit.* **2015**, *54*, 5560-5576.

26. Ohto, T.; Backus, E. H. G.; Hsieh, C.-S.; Sulpizi, M.; Bonn, M.; Nagata, Y., Lipid Carbonyl Groups Terminate the Hydrogen Bond Network of Membrane-Bound Water. *J. Phys. Chem. Lett.* **2015**, *6*, 4499-4503.
27. Watry, M. R.; Tarbuck, T. L.; Richmond, G. L., Vibrational Sum-Frequency Studies of a Series of Phospholipid Monolayers and the Associated Water Structure at the Vapor/Water Interface. *J. Phys. Chem. B* **2003**, *107*, 512-518.
28. Miranda, P. B.; Du, Q.; Shen, Y. R., Interaction of Water with a Fatty Acid Langmuir Film. *Chem. Phys. Lett.* **1998**, *286*, 1-8.
29. Gragson, D. E.; McCary, B. M.; Richmond, G. L., Surfactant/Water Interactions at the Air/Water Interface Probed by Vibrational Sum Frequency Generation. *J. Phys. Chem.* **1996**, *100*, 14272-14275.
30. Bell, G. R.; Bain, C. D.; Ward, R. N., Sum-Frequency Vibrational Spectroscopy of Soluble Surfactants at the Air/Water Interface. *J. Chem. Soc., Faraday Trans.* **1996**, *92*, 515-523.
31. Livingstone, R. A.; Nagata, Y.; Bonn, M.; Backus, E. H. G., Two Types of Water at the Water-Surfactant Interface Revealed by Time-Resolved Vibrational Spectroscopy. *J. Am. Chem. Soc.* **2015**, *137*, 14912-14919.
32. Nihonyanagi, S.; Yamaguchi, S.; Tahara, T., Direct Evidence for Orientational Flip-Flop of Water Molecules at Charged Interfaces: A Heterodyne-Detected Vibrational Sum Frequency Generation Study. *J. Chem. Phys.* **2009**, *130*, 204704.
33. Pool, R. E.; Versluis, J.; Backus, E. H. G.; Bonn, M., Comparative Study of Direct and Phase-Specific Vibrational Sum-Frequency Generation Spectroscopy: Advantages and Limitations. *J. Phys. Chem. B* **2011**, *115*, 15362-15369.
34. Inoue, K.-i.; Singh, P.; Nihonyanagi, S.; Yamaguchi, S.; Tahara, T., In *Ultrafast Phenomena Xix*, Yamanouchi, K.; Cundiff, S.; de Vivie-Riedle, R.; Kuwata-Gonokami, M.; DiMauro, L., Eds. Springer International Publishing: 2015; Vol. 162, pp 309-312.
35. Roy, S.; Gruenbaum, S. M.; Skinner, J. L., Theoretical Vibrational Sum-Frequency Generation Spectroscopy of Water near Lipid and Surfactant Monolayer Interfaces. *J. Chem. Phys.* **2014**, *141*, 18C502.
36. Sovago, M.; Campen, R. K.; Wurpel, G. W.; Müller, M.; Bakker, H. J.; Bonn, M., Vibrational Response of Hydrogen-Bonded Interfacial Water Is Dominated by Intramolecular Coupling *Phys. Rev. Lett.* **2008**, *100*, 173901.
37. Nagata, Y.; Mukamel, S., Vibrational Sum-Frequency Generation Spectroscopy at the Water/Lipid Interface: Molecular Dynamics Simulation Study. *J. Am. Chem. Soc.* **2010**, *132*, 6434-6442.
38. Mondal, J. A.; Nihonyanagi, S.; Yamaguchi, S.; Tahara, T., Structure and Orientation of Water at Charged Lipid Monolayer/Water Interfaces Probed by Heterodyne-Detected Vibrational Sum Frequency Generation Spectroscopy. *J. Am. Chem. Soc.* **2010**, *132*, 10656-10657.
39. Bredenbeck, J.; Ghosh, A.; Smits, M.; Bonn, M., Ultrafast Two Dimensional-Infrared Spectroscopy of a Molecular Monolayer. *J. Am. Chem. Soc.* **2008**, *130*, 2152.
40. Zhang, Z.; Piatkowski, L.; Bakker, H. J.; Bonn, M., Ultrafast Vibrational Energy Transfer at the Water/Air Interface Revelaed by Two-Dimensional Surface Vibrational Spectroscopy *Nat. Chem.* **2011**, *3*, 888-893.
41. Singh, P. C.; Nihonyanagi, S.; Yamaguchi, S.; Tahara, T., Ultrafast Vibrational Dynamics of Water at a Charged Interface Revealed by Two-Dimensional Heterodyne-Detected Vibrational Sum Frequency Generation. *J. Chem. Phys.* **2012**, *137*, 094706.
42. Xiong, W.; Laaser, J. E.; Mehlenbacher, R. D.; Zanni, M. T., Adding a Dimension to the Infrared Spectra of Interfaces Using Heterodyne Detected 2D Sum-Frequency Generation (HD 2D SFG) Spectroscopy. *Proc. Natl. Acad. Sci. U.S.A.* **2011**, *108*, 20902-20907.
43. Singh, P. C.; Nihonyanagi, S.; Yamaguchi, S.; Tahara, T., Communication: Ultrafast Vibrational Dynamics of Hydrogen Bond Network Terminated at the Air/Water Interface: A Two-Dimensional Heterodyne-Detected Vibrational Sum Frequency Generation Study. *J. Chem. Phys.* **2013**, *139*, 161101.
44. Hsieh, C.-S.; Okuno, M.; Hunger, J.; Backus, E. H. G.; Nagata, Y.; Bonn, M., Aqueous Heterogeneity at the Air/Water Interface Revealed by 2D-HD-SFG Spectroscopy. *Angew. Chem. Int. Edit.* **2014**, *53*, 8146-8149.
45. Post, S. T. v. d.; Hsieh, C.-S.; Okuno, M.; Nagata, Y.; Bakker, H. J.; Bonn, M.; Hunger, J., Strong Frequency Dependence of Vibrational Relaxation in Bulk and Surface Water Reveals Sub-Picosecond Structural Heterogeneity. *Nat. Commun.* **2015**, *6*, 8384.
46. Please note that the 2D-SFG spectra and the conclusion presented by some of us in J. Chem. Phys. 135 (2011) 021101 are different due to an improved measurement scheme and analysis of the spectra presented here. Moreover, the current data have better signal-to-noise ratio due to improved stability in the experimental setup.
47. Piatkowski, L.; Zhang, Z.; Backus, E. H. G.; Bakker, H. J.; Bonn, M., Extreme Surface Propensity of Halide Ions in Water. *Nat. Commun.* **2014**, *5*, 4083.
48. Yang, M., Validity of Förster Theory for Vibrational Energy Transfer in Low-Dimensional Water. *J. Phys. Chem. B* **2015**, *119*, 15516-15521.
49. Nicodemus, R. A.; Corcelli, S. A.; Skinner, J. L.; Tokmakoff, A., Collective Hydrogen Bond Reorganization in Water Studied with Temperature-Dependent Ultrafast Infrared Spectroscopy *J. Phys. Chem. B* **2011**, *115*, 5604-5616.
50. Fenn, E. E.; Wong, D. B.; Giammanco, C. H.; Fayer, M. D., Dynamics of Water at the Interface in Reverse Micelles: Measurements of Spectral Diffusion with Two-Dimensional Infrared Vibrational Echoes *J. Phys. Chem. B* **2011**, *115*, 11658-11670.
51. Chen, X.; Hua, W.; Huang, Z.; Allen, H. C., Interfacial Water Structure Associated with Phospholipid Membranes Studied by Phase-Sensitive Vibrational Sum Frequency Generation Spectrosopcy *J. Am. Chem. Soc.* **2010**, *132*, 11336-11342.
52. Costard, R.; Levinger, N. E.; Nibbering, E. T. J.; Elsaesser, T., Ultrafast Vibrational Dynamics of Water Confined in Phospholipid Reverse Micelles *J. Phys. Chem. B* **2012**, *116*, 5752-5759.
53. Lawrence, C. P.; Skinner, J. L., Vibrational Spectroscopy of HOD in Liquid D_2O. VI. Intramolecular and Intermolecular Vibrational Energy Flow. *J. Chem. Phys.* **2003**, *119*, 1623-1633.
54. Post, S. T. v. d.; Bakker, H. J., The Combined Effect of Cations and Anions on the Dynamics of Water. *Phys. Chem. Chem. Phys.* **2012**, *14*, 6280-6288.
55. Rezus, Y.; Bakker, H., On the Orientational Relaxation of Hdo in Liquid Water. *J. Chem. Phys.* **2005**, *123*, 114502-114502.
56. Lindner, J.; Vöhringer, P.; Pshenichnikov, M. S.; Cringus, D.; Wiersma, D. A.; Mostovoy, M., Vibrational Relaxation of Pure Liquid Water. *Chem. Phys. Lett.* **2006**, *421*, 329-333.
57. Ghosh, A.; Smits, M.; Bredenbeck, J.; Bonn, M., Membrane-Bound Water Is Energetically Decoupled from Nearby Bulk Water: An Ultrafast Surface-Specific Investigation. *J. Am. Chem. Soc.* **2007**, *129*, 9608–9609.
58. Bodis, P.; Larsen, O. F. A.; Woutersen, S., Vibrational Relaxation of the Bending Mode of HDO in Liquid D_2O. *J. Phys. Chem. A* **2005**, *109*, 5303-5306.
59. Bredenbeck, J.; Ghosh, A.; Nienhuys, H.-K.; Bonn, M., Interface-Specific Ultrafast Two-Dimensional Vibrational Spectroscopy. *Accounts Chem. Res.* **2009**, *42*, 1332-1342.
60. Kroh, D.; Ron, A., The Overtone Spectra of H2o, D2o and Mixtures of H2o in D2o Ice. *Chem. Phys. Lett.* **1975**, *36*, 527-530.
61. Kropman, M. F.; Nienhuys, H. K.; Woutersen, S.; Bakker, H. J., Vibrational Relaxation and Hydrogen-Bond Dynamics of HDO:H_2O. *J. Phys. Chem. A* **2001**, *105*, 4622-4626.
62. Asbury, J. B.; Steinel, T.; Kwak, K.; Corcelli, S. A.; Lawrence, C. P.; Skinner, J. L.; Fayer, M. D., Dynamics of Water Probed with Vibrational Echo Correlation Spectroscopy *J. Chem. Phys.* **2004**, *121*, 12431-12446.

63. Hamm, P.; Helbing, J.; Bredenbeck, J., Stretched Versus Compressed Exponential Kinetics in α-Helix Folding. *Chem. Phys.* **2006**, *323*, 54-65.
64. Kundu, A.; Kwak, K.; Cho, M., Water Structure at the Lipid Multibilayer Surface: Anionic Versus Cationic Head Group Effects. *J. Phys. Chem. B* **2016**, *120*, 5002-5007.
65. Singh, P. C.; Inoue, K.-i.; Nihonyanagi, S.; Yamaguchi, S.; Tahara, T., Femtosecond Hydrogen Bond Dynamics of Bulk-Like and Bound Water at Positively and Negatively Charged Lipid Interfaces Revealed by 2d HD-VSFG Spectroscopy. *Angew. Chem. Int. Edit.* **2016**, *128*, 1-6.

Table of contents image